Detailed structure of the hexagonally packed mesostructured carbon material CMK-3

L.A. Solovyov[a],*, A.N. Shmakov[b], V.I. Zaikovskii[b], S.H. Joo[c], R. Ryoo[c]

[a]*Institute of Chemistry and Chemical Technology, K. Marx Av. 42, Krasnoyarsk 660049, Russia*
[b]*Boreskov Institute of Catalysis, Novosibirsk 630090, Russia*
[c]*National Creative Research Initiative Center for Functional Nanomaterials and Department of Chemistry
(School of Molecular Science-BK21), Korea Advanced Institute of Science and Technology, Taejon 305-701, South Korea*

Abstract

Detailed investigation of the ordered mesoporous CMK-3 carbon using XRD structural modeling based on the continuous electron density representation and the Rietveld technique allowed deriving comprehensive and consistent information on the material anatomy. The electron density distribution map agrees with carbon 'bridges', which seem to be attributed to the material interconnecting carbon nanorods in the CMK-3 mesostructure. These carbon 'bridges' are supposed to be derived from former complementary mesopores of the SBA-15 template used.
© 2002 Elsevier Science Ltd. All rights reserved.

Keywords: A. Mesophase; B. Impregnation; Carbonization; C. Electron microscopy; X-ray diffraction

1. Introduction

Recently, new types of mesostructured carbon materials have been synthesized using mesostructured silica templates, and the most important physico-chemical properties of these materials have been described [1]. As it was demonstrated [2–5], the template needs to have either three-dimensionally interconnected or interwoven pore structure in order to be suitable for the mesostructured carbon synthesis, otherwise disordered microporous carbon is formed. In particular, application of pure siliceous SBA-15 type template in the synthesis leads to hexagonally packed mesostructured carbon replica (referred to as CMK-3) [3,4]. Typically, the SBA-15 template was prepared at 35 °C under strong acidic conditions (pH ≪ 1) with following hydrothermal aging for a few days at a temperature in the range of 80–100 °C [6,7]. The structure of the template thus synthesized was proved to include, except primary (structural) mesopores of about 9–10 nm in diameter, a significant fraction of complementary mesopores of the

size in an approximate range from 1 to 3 nm, the latter being inferred to provide connectivity between the primary mesopores of SBA-15 [6,8]. This identification of the SBA-15 template structure as having three-dimensional pore system facilitated the synthesis of the ordered mesoporous carbons CMK-3, whose structure was a faithful replica of the ordered silica template. As shown by high-resolution TEM [3], the CMK-3 material consisted of uniformly sized carbon rods arranged in a hexagonal pattern. At the same time, the arrangement of connections between these rods was not clarified yet. In this work we undertook detailed investigation of the CMK-3 material using earlier developed structural modeling approach based on the continuous electron density representation [9] and the Rietveld technique [10].

2. Experimental

The CMK-3 material was synthesized according to the procedure, which has been already described [3].

X-ray diffraction measurements were performed on a precise diffractometer of high resolution, which is located in Siberian Center of Synchrotron Radiation. Having installed the Ge(111) plane perfect crystal analyzer on the

*Corresponding author. Tel.: +7-3912-495-663; fax: +7-3912-238-658.
E-mail address: leosol@krsk.info (L.A. Solovyov).

diffracted beam, high natural collimation of the synchrotron beam in the vertical plane provides high instrumental resolution of the diffractometer. As a result, an instrumental half-width of the XRD reflections is permitted to be diminished up to $\Delta(2\theta)\sim0.04°$ in the low-angle region of $1–7°$ 2θ. Vertical parallel Soller's collimator with a 5-mrad divergence was applied to restrict azimuth divergence of the diffracted beam and to reduce low-angle peak asymmetry. The Si(111) crystal-monochromator provides the monochromatization degree of the radiation up to $\Delta\lambda/\lambda\sim10^{-4}$. Additionally, X-ray diffraction data were collected on a laboratory diffractometer (DRON-4, Cu Kα radiation) with a primary beam collimator and a secondary flat graphite monochromator. The measurements were performed in the transmission mode. The laboratory setup was used to carry out precise measurements of peak intensities, which were necessary for structural investigations. Scanning was performed under ambient conditions over the 2θ region from 0.5 to 5° at steps of 0.04° 2θ and accumulation time 100 s/step.

TEM images were obtained in bright field mode on a JEM 2010 electron microscope having 0.14 nm instrumental resolution.

Structural modeling was fulfilled using the continuous electron density representation and the Rietveld full-profile technique. Corresponding data processing has been already described in detail [9].

3. Results and discussion

Transmission microscope images in both projections (parallel and perpendicular to the carbon rods, Fig. 1A,B, respectively) justify that the structure of the CMK-3 material under study is highly ordered hexagonal arrangement of these nanorods. As seen from the images, all the rods are of very close diameters and perfectly located in the structure. The HRTEM image of a single rod (Fig. 1C) allows observing its internal detailed structure. Carbon rod seems to consist of graphite-like structural fragments, which are packed in the rod disorderedly. Corresponding interlayer distances of about 0.35 nm, which are characteristic to the graphite structure, can be easily seen in the HRTEM image.

Synchrotron XRD pattern of the material (Fig. 2) exhibits three narrow peaks with a full-width-at-half maximum (FWHM) value close to the instrumental one. This indicates that not only the structure of the parts of the sample suitable for the TEM investigations may be characterized as highly ordered, but also the structure of the material as a whole has to be described as fairly long-range ordered hexagonal arrangement of carbon rods. Based on these synchrotron diffraction data, which provided high resolution and the least instrumental aberrations, the unit cell constant a_0 of the two-dimensional hexagonal lattice of the material was determined to be 9.66(1) nm.

(a)   **(b)**   **(c)**
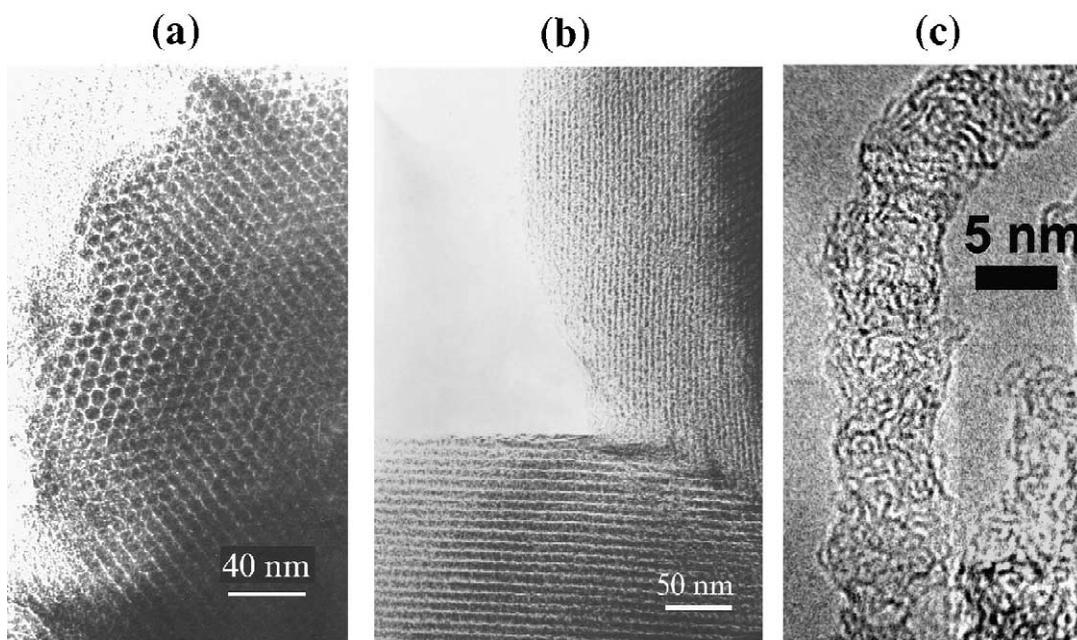
40 nm   50 nm   5 nm

Fig. 1. Transmission electron microscopy images of the CMK-3 material studied. (a) Projection along the direction, parallel to carbon rods; (b) projections along the direction, perpendicular to carbon rods; (c) HRTEM image of a single carbon rod.
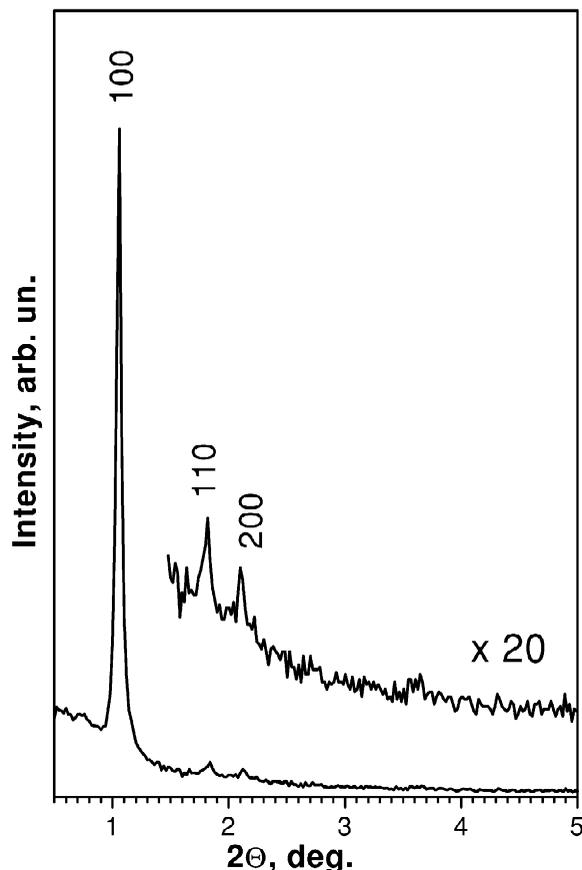
Fig. 2. Synchrotron X-ray diffraction pattern for the CMK-3 material studied.
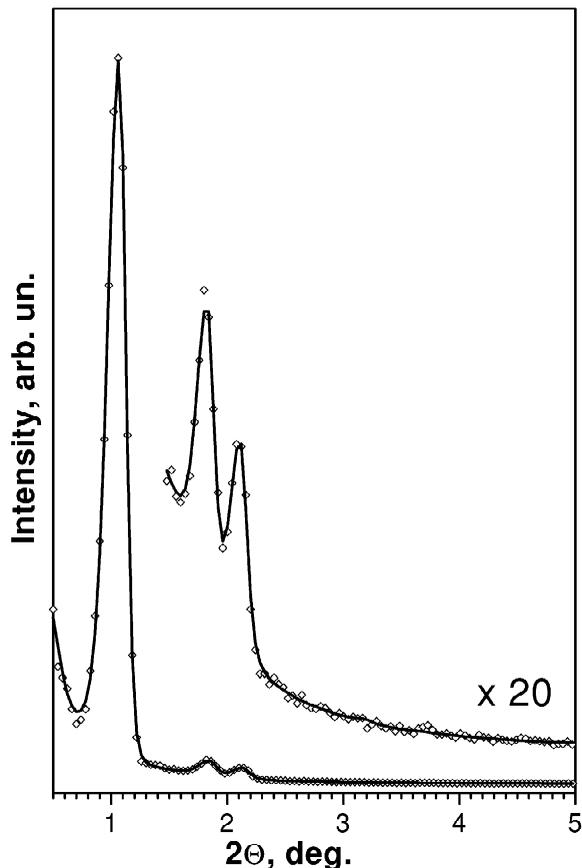

Fig. 3. Experimental (dots, obtained on the laboratory setup) and calculated (solid line) X-ray powder patterns for the CMK-3 material after the structure refinement. The background line is partly corrected for better view.

As the powder patterns of the material revealed only three appreciably nonzero peaks, the structure model was confined to be as simple as possible. The density distribution was represented by a hexagonal array of cylinders with adjustable diameter D having constant density. The dispersal of the cylinder edges was simulated by application of the exponential correction with variable isotropic temperature factor B_{iso}. This correction, also referred as the Debye–Waller factor, is used in X-ray crystallography for taking into account atomic thermal vibration and disordering. The refinement of the structure parameters D and B_{iso} by means of the continuous density approach and the Rietveld full-profile technique led to the following values: $D=7.1(1)$ nm; $B_{iso}=45(5)$ nm^2.

The experimental and calculated powder diffraction patterns after the structure refinement are shown in Fig. 3. Individual intensities, structure factors and calculated initial phases of the first 10 reflections are listed in Table 1. The experimental intensities of the first three reflections

Table 1
Experimental and calculated intensities, structure factor modules and initial phases for the first 10 reflections

(*hkl*)	I_{obs}	I_{calc}	$\lvert F_{obs}\rvert$	$\lvert F_{calc}\rvert$	Phase
100	1 000 157	1 000 000	100.08	100.00	0
110	18 905	18 696	23.80	23.67	π
200	13 095	13 406	22.87	23.14	π
210	–	16	–	0.74	0
300	–	180	–	4.02	0
220	–	34	–	2.01	0
310	–	13	–	0.96	0
400	–	1	–	0.43	π
320	–	2	–	0.53	π
410	–	>1	–	0.28	π

were evaluated from the powder pattern using the Le Bail algorithm [11,12]. The remaining reflections could not be explicitly resolved from noise. As it can be seen from Fig. 3 and Table 1, expected intensities of all the reflections except (100), (110) and (200) must be really negligible. Therefore, one may conclude that all the basic accessible information on the density distribution in the material studied is contained in the first three reflections. The final reliability factors of the refinement, characterizing the disagreement between the experimental and calculated intensities and structure factors [11], are $R_I=0.07\%$ and $R_F=0.33\%$. These values indicate that the structure model chosen provides an exhaustive fit to the experimental data, varying two structural parameters only.

The electron density distribution map obtained using the experimental intensities (Fig. 3) and calculated initial phases (Table 1) is shown in Fig. 4. It demonstrates an array of essentially circular dispersed areas of constant density. This array corresponds, obviously, to the carbon rods, and is in accordance with the refined structure model. The dispersal of the areas is rather broad, which is also reflected in very high value of B_{iso}. This value may, surely, be attributed not only to the positional disordering of the carbon nanorods, but also to their surface roughness corresponding to that of the SBA-15 silica channels [8]. Structural characteristics of the CMK-3 material are schematically inscribed into the map of electron density distribution for this material (Fig. 4). The value 7.1 nm of the mean diameter of the carbon nanorods obtained from the structure refinement is in a good agreement with both current TEM observations (Fig. 1A,C) and recently reported value of 7 nm for the same material [3].

Between the areas one can see some 'bridges' of non-zero density, which seem to be attributed to the material interconnecting the rods. These local maximums on the
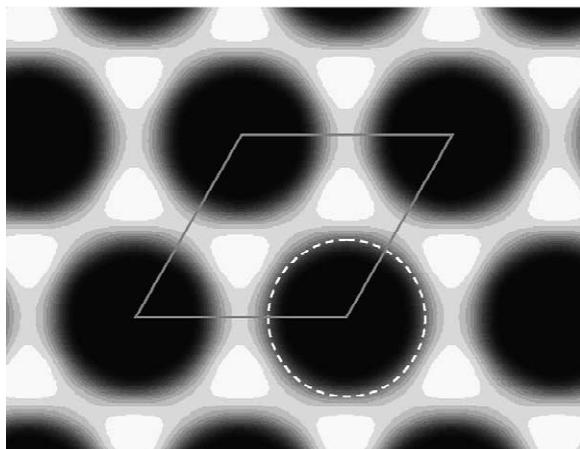

Fig. 4. Electron density distribution map for the CMK-3 material. The unit cell is outlined by solid lines. The dashed circle corresponds to the diameter of 7.1 nm.

density map cannot be interpreted as a noise that might arise due to finite number of structure factors involved in the calculation. The bridge areas have peak height of 20% of the density within the carbon rod areas and width of about 3 nm. Such bulk features cannot be compensated by involving the remaining reflections in the calculation, which were shown to have negligible structure factors (see Table 1 and Fig. 3). While the density map calculation was performed on the basis of only three experimental reflections (or nine structure factors including symmetry-equivalents), the simplicity of the structure model and the density distribution obtained are quite adequate to the number of observations. Since the d-spacing of the last reflection is 4.2 nm, the expected density map resolution can be estimated as 2 nm. This resolution is as well adequate to the breadth of the considered bridge density areas.

The carbon 'bridges' observed on the density map are supposed to be derived from former complementary porosity of the SBA-15 template used. The complementary pores were inferred to provide connectivity between the primary (structural) mesopores of SBA-15 [6]. Therefore, being involved into the syntheses of carbon derivatives, such three-dimensional structure of the SBA-15 template leads to the formation of hexagonal array of carbon rods (derived from former primary mesopores), which is interconnected with the carbon bridges derived from former complementary porosity.

4. Conclusion

The combined TEM and XRD structural modeling of the mesostructured carbon molecular sieve CMK-3 allowed characterization of the material as a fairly long-range ordered hexagonal arrangement of carbon nanorods. The XRD structural modeling based on the continuous electron density representation and the Rietveld technique showed that the nanorods were essentially circular and had average diameter of 7.1(1) nm which was consistent with both TEM and adsorption data. The electron density distribution map for the material revealed some 'bridges' of non-zero density between the cylinders which could be attributed to the carbon material providing their connectivity derived from former complementary porosity of the SBA-15 mesoporous template.

References

[1] Ryoo R, Joo SH, Kruk M, Jaroniec M. Ordered mesoporous carbons. Adv Mater 2001;13(9):677–861.

[2] Kruk M, Jaroniec M, Ryoo R, Joo SH. Characterization of ordered mesoporous carbons synthesized using MCM-48 silicas as templates. J Phys Chem B 2000;104(33):7960–8.

[3] Jun S, Joo SH, Ryoo R, Kruk M, Jaroniec M, Liu Z, Ohsuna T, Terasaki O. Synthesis of new nanoporous carbon with hexagonally ordered mesostructure. J Am Chem Soc 2000;122(43):10712–3.

[4] Shin HJ, Ryoo R, Kruk M, Jaroniec M. Modification of SBA-15 pore connectivity by high-temperature calcination investigated by carbon inverse replication. Chem Commun 2001:349–50.

[5] Lee J, Yoon S, Oh SM, Shin C, Hyeon T. Development of a new mesoporous carbon using an HMS aluminosilicate template. Adv Mater 2000;12(5):359–62.

[6] Kruk M, Jaroniec M, Ko CH, Ryoo R. Characterization of the porous structure of SBA-15. Chem Mater 2000;12(7):1961–8.

[7] Zhao D, Feng J, Huo Q, Melosh N, Fredrickson GH, Chmelka BF, Stucky GD. Triblock copolymer syntheses of mesoporous silica with periodic 50 to 300 Angstrom pores. Science 1998;279(1):548–52.

[8] Liu Z, Terasaki O, Ohsuna T, Hiraga K, Shin HJ, Ryoo R. HREM study of channel structure of silica mesoporous SBA-15 and Pt wires produced in the channels. Chem Phys Chem 2001;2(4):229–31.

[9] Solovyov LA, Kirik SD, Shmakov AN, Romannikov VN. X-ray structural modeling of silicate mesoporous mesophase material. Micropor Mesopor Mater 2001;44–45:17–23.

[10] Rietveld HM. Profile refinement method for nuclear and magnetic structures. J Appl Crystallogr 1969;2(2):65–71.

[11] McCusker LB, VonDreele RB, Cox DE, Louer D, Scardi P. Rietveld refinement guidelines. J Appl Crystallogr 1999;32(1):36–50.

[12] Le Bail A, Duroy H, Fourquet JL. Ab-initio structure determination of $LiSbWO_6$ by X-ray powder diffraction. Mater Res Bull 1988;23(5):447–52.